Alternative Approach to Estimate Lumped Constant in the Deoxyglucose Model: Simulation and Validation

Hiroshi Matsuda,* Hirofumi Nakai, Sayed Jovkar, Mirko Diksic, Alan C. Evans, Ernst Meyer, Christoph Redies, and Y. Lucas Yamamoto

Cone Laboratory for Neurosurgical Research, Montreal Neurological Institute and Hospital, and Department of Neurology and Neurosurgery, McGill University, Montreal, Quebec, Canada

An alternative method of estimating the lumped constant (LC) in the deoxyglucose model was developed. The LC was estimated using data obtained during the first 10 min after injection of the tracer by a nonlinear least-squares (NLSQ) method. The method does not require a constant plasma concentration. This approach was evaluated in a computer simulation by adding different levels of noise and considering various input functions. Errors in the estimated LC in this and Sokoloff et al.'s conventional method were compared. We found that the approach proposed here results in more reliable estimates of LC. The study is completed in a shorter experimental period, and any shape of the input function can be used. The new technique was then applied to measure whole brain LC and rate constants in cat brain for 2-[^{18}F]fluoro-2-deoxy-D-glucose (2-[^{18}F]FDG). Measured mean value (±s.e.m.) for the whole brain LC = 0.443 ± 0.012 (N = 7), for the whole brain k_2^* = 0.124 ± 0.009 and k_3^* = 0.024 ± 0.001 (N = 7).

J Nucl Med 28:471–480, 1987

The quantitative measurement of regional glucose utilization by the deoxyglucose method was introduced by Sokoloff et al. (*1*), who determined the lumped constant (LC) as the mean of the individual asymptotic values of the ratio of deoxyglucose and glucose extraction fraction multiplied by specific activities. This approach requires a constant arterial plasma tracer concentration. The LC values vary not only with the species of animal (*1,2*), but also with analog used (*3*) and pathologic conditions such as ischemia (*4,5*) or hypoglycemia (*6,7*). The Sokoloff method (*1*) is based on the assumption that the rate constant for dephosphorylation of deoxyglucose phosphate (k_4^*) is zero. If k_4^* is not zero, then the extraction ratios do not converge to a constant value. A large series of animals is required to reduce the margin for analytic errors (*1*). In pathologic conditions such as hyperglycemia (*8*) or ischemia (*9*), where the precursor pool has a slow turnover, the time needed to reach the asymptotic value could be longer than the proposed experimental period of 45 min (*1*). Maintaining the arterial plasma concentration of a tracer constant during an experiment is not always easily accomplished (*4,10,11*).

An alternative method is proposed to improve the LC measurements. Since over a short experimental period the loss of deoxyglucose phosphate, if any, from the tissue could be assumed to be negligible (*12,13*), a shorter experimental period (10 min) should give more accurate results. An improvement is also seen in the method for the LC measurements because it does not require a constant arterial plasma concentration of the tracer.

The present study was carried out to develop an alternative approach for measuring LC. Various input functions were compared using a computer simulation and then tested in the cat.

MATERIALS AND METHODS

Simulation Study

In simulation studies, the influence of different levels of random noise on the determination of LC was evaluated,

Received Jan. 28, 1986; revision accepted Sept. 4, 1986.

For reprints contact: Mirko Diksic, PhD or Lucas Y. Yamamoto, MD, PhD, Montreal Neurological Institute, 3801 University St., Montreal, Quebec, H3A 2B4 Canada.

* Dr. Matsuda was on leave of absence from the Department of Nuclear Medicine, Kanazawa University Hospital, 13-1, Takara-machi, Kanazawa, Ishikawa 920, Japan.

(Random noise was chosen as the best representative of experimental errors influencing measured parameters.) Various experimental protocols with different arterial plasma concentration curves (input function) and different methods of analysis were evaluated.

All integrals were calculated by numerical integration using a spline approximation (*14*).

Tracer Concentration in Arterial Plasma, $C_p^*(t)$

1. The constant $C_p^*(t)$ model was defined as one with a constant arterial plasma concentration. Constant $C_p^*(t)$ was obtained using the infusion schedule controlled by a microcomputer according to the method described before by Patlak and Pettigrew (*11*).

2. Since physiological conditions generally vary from time to time and from animal to animal, the transfer function (T(t)) obtained from a bolus done in one animal may not be applicable to others. To simulate the individual effect of each parameter of T(t) expressed as a sum of three exponential curves on the resulting $C_p^*(t)$, several versions of $C_p(t)$ were generated by using a modified form of T(t) in each case. For each version of T(t), all parameters were identical to those originally determined. The exception was the parameter that was changed by +100% or −50%.

The $C_p^*(t)$ was generated at intervals of 1 min for the first 10 min and then every 2 min from 12 to 44 min. Random noise was added to the $C_p^*(t)$, resulting in an input function $C_p^{*\prime}(t)$. Random numbers were selected from a normal distribution with standard deviation proportional to the function value (*14*). In other words, the noise level of Z% added to the function value F was a random number drawn from a normal distribution with zero mean and standard deviation FZ/100.

Tracer Concentration in Arterial Blood, $C_a^*(t)$

$C_a^*(t)$ was generated from $C_p^*(t)$ and the experimentally measured ratios of the tracer concentration in arterial blood to that in the arterial plasma, as a function of time ($C_p^*(t) = 0.004 \cdot C_a^*(t) + 0.566$). Random noise was added to $C_a^*(t)$ to generate $C_a^{*\prime}(t)$ as mentioned above for $C_p^{*\prime}(t)$.

Tracer Concentration in Draining Venous Blood, $C_v^*(t)$

Having $C_p/(C_a - C_v)$ in Eq. A12 set to 10 (ten was used because the experimental values were close to it) and solving it for $C_v^*(t)$ yields

$$C_v^*(t) = C_a^*(t) - \frac{LC\left(1 + \frac{k_2^*}{k_3^*}\right)\left[C_p^*(t) - \frac{(Ae^{-\alpha_1 t} - Be^{-\alpha_2 t})}{\alpha_2 - \alpha_3} \otimes C_p^*(t)\right]}{10}. \quad (1)$$

Again, an addition of random noise to $C_v^*(t)$ resulted in $C_v^{*\prime}(t)$ as described above. The values for k_2^* and k_3^* were set to 0.245 and 0.052 (*1*), respectively, and three values were chosen for the "true" value of LC, namely 0.8, 0.48, and 0.25. The effect of k_4^* on the resulting g(t) was evaluated by repeating calculations using four different values of k_4^*: 0, 0.005, 0.01, and 0.02.

LC Determination

The expression for g(t) with noise added [(g′(t)] was generated at each sampling time:

$$g'(t) = \frac{C_p[C_a^{*\prime}(t) - C_v^{*\prime}(t)]}{C_p^*(t)\,(C_a - C_v)}, \quad (2)$$

assuming $C_p/(C_a - C_v)$ to be equal to 10.

Substituting k_4^* equal to zero, Eq. A12 becomes

$$g'(t) = LC'(1 + C) \cdot \left[1 - \frac{CD/(1 + C)\, e^{-Dt} \int_0^t e^{D\tau} C_p^{*\prime}(\tau)d\tau}{C_p^{*\prime}(t)}\right], \quad (3)$$

where

$$C = k_2^{*\prime}/k_3^{*\prime} \text{ and } D = k_2^{*\prime} + k_3^{*\prime}.$$

The data for g′(t) were fitted to Eq. (3) by a nonlinear least squares (NLSQ) method (*15*) to obtain values for LC′, C, and D using the VAX 11/750 computer (DEC). This also permitted the calculation of $k_2^{*\prime}$ and $k_3^{*\prime}$.

LC′ was defined as the average of ten g′(t) values between 26 to 44 min to approximate the Sokoloff method as the estimated LC value.

The errors in percent for LC′, LC″, $k_2^{*\prime}$, and $k_3^{*\prime}$ as compared to the true LC, k_2^*, and k_3^* are calculated as follows:

$$\delta LC'(\%) = 100(LC' - LC)/LC \quad (4)$$

$$\delta LC''(\%) = 100(LC' - LC)/LC \quad (5)$$

$$\delta k_2^{*\prime}(\%) = 100(k_2^{*\prime} - k_2^*)/k_2^* \quad (6)$$

$$\delta k_3^{*\prime}(\%) = 100(k_3^{*\prime} - k_3^*)/k_3^*. \quad (7)$$

ANIMAL STUDY

Animal Preparation

The studies were done on five male and two female adult cats weighing 3.4 to 4.3 kg. The animals were provided with water *ad libitum*, but deprived of food for ~18 hr before the experiment. Before surgical preparation the animals were anesthetized by intraperitoneal injection of sodium pentobarbital (40 mg/kg). After tracheotomy, respiration was controlled by a Mark 6 ventilator+ with medical air and 1.0% halothane. Body temperature was maintained with a thermostatically controlled heating blanket at physiological levels (36.5°C). The right femoral artery and vein and a branch of the left femoral vein were cannulated with polyethylene tubes (PE 90 for the femoral artery and vein, and PE 50 for the branch of the femoral vein) for administration of tracer and for measuring the radioactivity of arterial blood and plasma, blood gas, and blood pressure. The superior sagittal sinus was exposed in the caudal portion of the coronal suture, and cannulated with a PE 50. This cannula was fixed to the dura using cyanoacrylated glue and gel-foam. After finishing all surgical procedures, anesthesia was changed to i.v. ketamine hydrochloride (20 mg/kg). For muscle paralysis, gallamine (2 mg/kg) was given at 1-hr intervals.

Physiological variables were as follows: mean arterial blood pressure: 117 ± 13 mmHg (mean ± s.d.), pH: 7.33 ± 0.5, $PaCO_2$: 35 ± 2 mmHg, PaO_2: 111 ± 13 mmHg, body temperature: 36.6 ± 0.5°C.

Types of Infusion of Tracer and Blood Sampling Schedule

The influence of different input functions on the final result was evaluated by selecting four types of tracer infusion and

blood sampling schedule. The input functions were classified according to their shape.

In four cats, $Cp^*(t)$ was maintained constant by the method of Patlak and Pettigrew (*11*). The transfer function [T(t)] for each cat was obtained by injecting a bolus of 30 μCi of [^{3}H]2-deoxy-D-glucose‡ (DG, specific activity 45–55 mCi/μmol) into the femoral vein. Blood samples were taken from the femoral artery at various times up to 47 min after the injection. Plasma was separated from these samples by centrifugation (1 min at 12,500 *g*) and analyzed for radioactivity by liquid scintillation. The parameters defining T(t) were determined using a nonlinear least squares fitting method (*16*).

According to the infusion schedule determined from the transfer function (see Appendix for details), 3 to 6 mCi of 2-fluorine-18-fluoro-2-deoxy-D-glucose (2-[^{18}F]FDG) dissolved in 6 ml of physiological saline were infused. Fluorine-18-labeled 2-FDG was prepared by adapting methods described in detail elsewhere (*17,18*). From this volume, 4.5 ml was continuously infused into the femoral vein using a calibrated

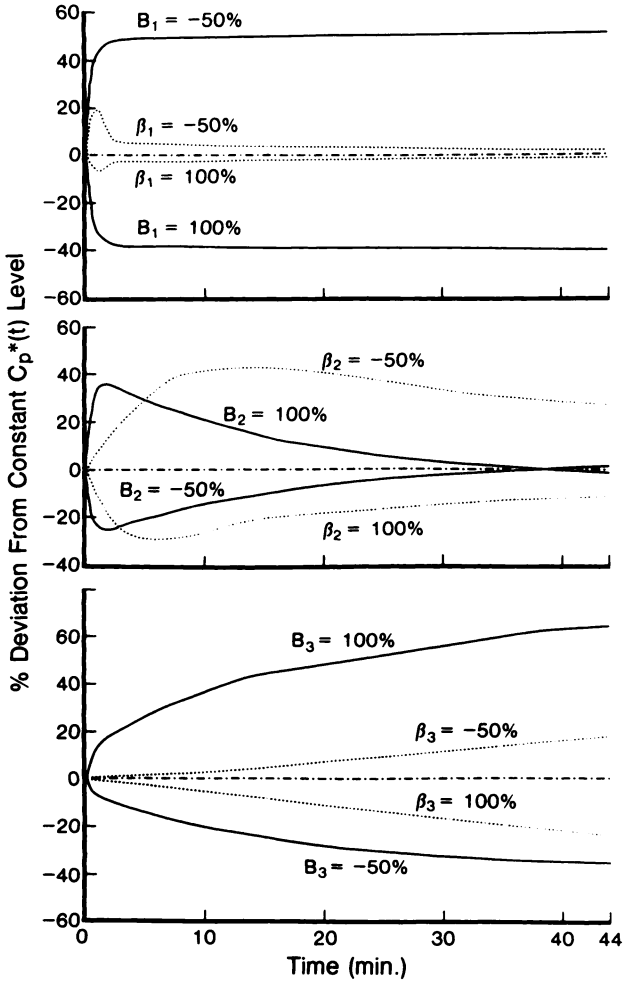

FIGURE 1
The $C_p^*(t)$ input functions generated by keeping all parameters of the transfer function identical, except for one parameter, to those used in deriving the constant $C_p^*(t)$ model infusion schedule (·–·). The variations of each parameter were a 100% increase and a 50% decrease. Top: Variations of B_1 and β_1. Middle: Variations of B_2 and β_2. Bottom: Variations of B_3 and β_3.

Harvard peristaltic pump controlled by an IBM microcomputer, and <1 ml was injected into the branch of the femoral vein as a bolus (delta function) (*11*). During the infusion, arterial and cerebral venous blood samples were taken from the femoral artery and the superior sagittal sinus, respectively. The sampling schedule was as follows: 1, 1.5, 2, 3, 4, 5, 6, 7, 8, 9, 10, 11, 12, 14, 18, 22, 27, 32, 38, and 45 min. The concentrations of 2-[^{18}F]FDG in the arterial plasma, arterial blood, and cerebral venous blood were determined by assay of [^{18}F]radioactivity in 50 μl of the sample using a well counter. Radioactivity was corrected for weight and decay by correcting values back to the start of infusion and expressed in μCi per gram. Plasma glucose concentration was enzymatically measured using a glucose analyzer.§

One cat was injected with 3 mCi of 2-[^{18}F]FDG dissolved in 3.5 ml of physiological saline, from which 3 ml was continuously infused according to a typical infusion schedule as described above. No tracer, however, was injected as a bolus. The following sampling schedule for arterial plasma was used: every 30 sec for the first 5, 6, 7, 8, 10, and 12 min. Eight pairs of arterial and cerebral venous blood samples were taken during the first 10 min.

In one cat, 5 mCi of 2-[^{18}F]FDG was dissolved in 1 ml of physiological saline and slowly injected for 30 sec. The sampling schedule for arterial plasma was as follows: every 15 sec for the first 2 min, every 30 sec for the next 3 min, and then every 6 min. Nine pairs of arterial and cerebral venous blood samples were taken during the first 5 min.

One cat received 1 mCi of 2-[^{18}F]FDG dissolved in 2 ml of physiological saline. Using the same pump as above, 1.5 ml of this was continuously infused at a constant rate. Arterial plasma was sampled: every 30 sec for the first 5 min, and then every 7, 9, and 11 min. Nine pairs of arterial and cerebral venous blood samples were taken during the first 10 min.

LC Calculation

The function g(t) described by Eq. (12) using $k_4^* = 0$ during the first 10 min was fitted by the same method as that used and described in the simulation study with the model Eq. (3), to get estimates for LC, k_2^*, and k_2^*.

RESULTS

Simulation Study

The transfer function, T(t), obtained from a bolus injection of 2-[^{3}H]DG was

$$T(t) = \sum_{i=1}^{3} \beta_i e^{-\beta_i t} \qquad (8)$$

$$= 0.691\ e^{-6.93t} + 0.243\ e^{-0.245t} + 0.065\ e^{-0.016t},$$

where t represents the difference between observed and lag time (*11*). Using this T(t), the $Cp^*(t)$ functions were generated by varied individual parameters of T(t) (Fig. 1). When B_i or β_i were varied, the $Cp^*(t)$ either gradually approached the steady-state level or had an initial overshoot (or undershoot) of the steady-state value before approaching the steady-state level. A variation in the B_2 or β_2 produced $C_p^*(t)$ with a maximum followed by a gradual decrease or a minimum followed by a gradual

increase (Fig. 1). In cases when B_3 or β_3 were varied, Cp*(t) either increased or decreased gradually throughout 44 min. An example of simulated Cp*(t), Ca*'(t), Cv*'(t) and g'(t) with random noise added is shown in Figure 2.

The influence of k_4^* on the resulting g(t) becomes large as measurements take a longer time or as the value of k_4^* increases (Fig. 3). The effect is <5%, however, when measurements are done during the first 10 min, even with k_4^* as high as 0.02.

The errors in estimates of LC', $k_2^{*\prime}$, and $k_3^{*\prime}$ when the NLSQ method was used are given in Figure 4 for various random noise levels and for various numbers of data points for g'(t) collected in a predetermined time period. The errors were evaluated using a constant Cp*(t) as the input function and setting LC, k_2^*, k_3^*, and k_4^* to 0.48, 0.245, 0.052, and 0.01, respectively. As shown in Figure 4, it seems that the error in the estimation of LC is lower or at least comparable using ten data sets in the first 10 min for all noise levels evaluated

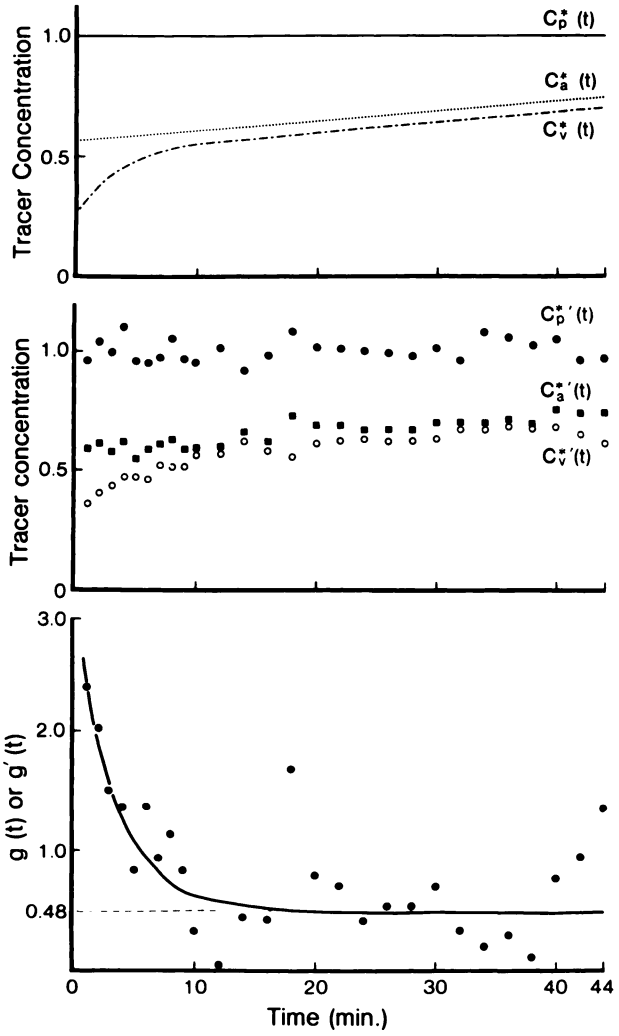

FIGURE 2
Examples of simulated $C_p^{*\prime}$(t), $C_a^{*\prime}$(t), $C_v^{*\prime}$(t) and g(t) functions assuming k_4^* equal to zero. Top: Noise-free C_p^*(t) (—), C_a^*(t) (——), and C_v^*(t) (·—·). Middle: 5% noise-added $C_p^{*\prime}$(t) (●), C_v^*(t) (○), Bottom: Noise-free g(t) (—) and 5% noise-added g'(t) (●). True LC, k_2^*, and k_3^* are 0.48, 0.245, and 0.052, respectively.

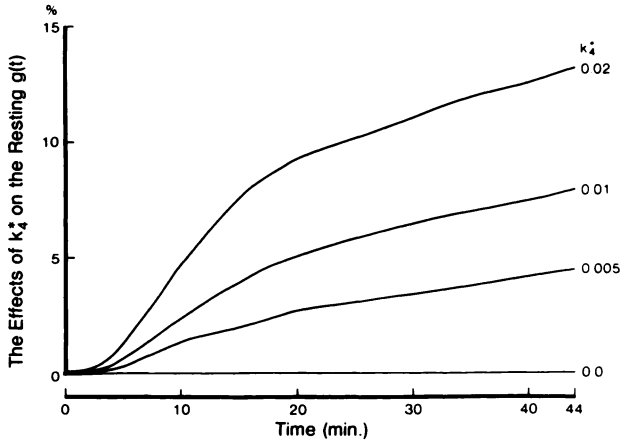

FIGURE 3
Effects of various values of k_4^* on the resulting g(t) as defined by Eq. (A12), expressed as the percent deviation from g(t) in which k_4^* was zero, $k_2^* = 0.245$; $k_3^* = 0.052$.

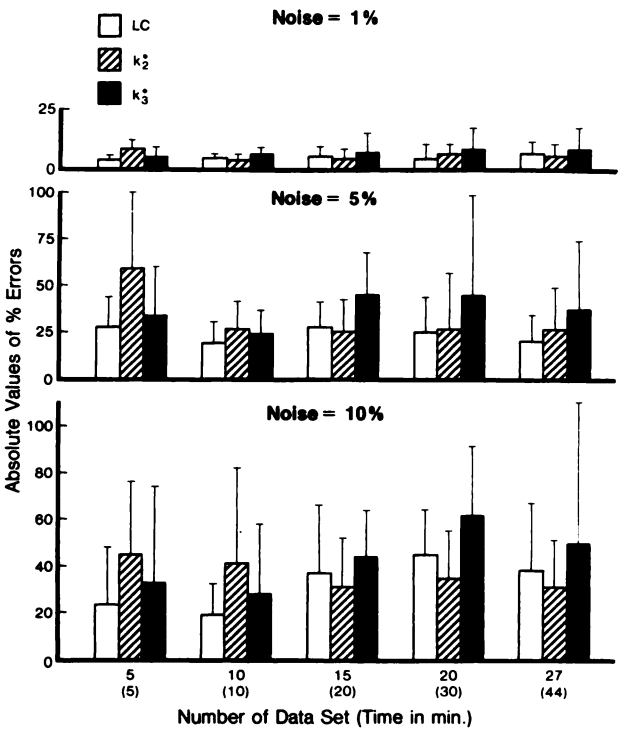

FIGURE 4
The relationship between the absolute values of the errors in LC', $k_2^{*\prime}$ and $k_3^{*\prime}$ values resulting from the NLSQ method, and different number of time-course data sets of g'(t) with a noise level of 1% (top), 5% (middle), and 10% (bottom) for the constant C_p^*(t) model, setting true LC, k_2^*, k_3^*, and k_4^* to 0.48, 0.245, 0.052, and 0.01, respectively. Column and bar represent mean and s.d. of absolute values of percent errors obtained from ten kinds of time course data sets of g'(t). In fitting 10 min data set χ_o^2 was 0.032, 0.137, and 0.552, when 1%, 5%, and 10% noise was added to the theoretical curve.

here. Consequently, it was concluded that the appropriate number of data sets should be around ten for the first 10 min.

The errors in LC′ and LC″, estimated from the NLSQ and the conventional methods, respectively, are compared in Table 1. Comparison is given for various random noise levels and three different "true" LC values for the constant Cp*(t) model. The LC′ was estimated from the model, setting $k_4^* = 0.01$ and applying a 10-min experimental protocol while the LC″ was calculated using k_4^* zero or 0.01. The errors become large as the noise level increases or as the "true" LC value decreases for both NLSQ and the conventional methods. In general, the NLSQ approach had smaller errors than the conventional method. In most cases the errors in the conventional method are higher when k_4^* was 0.01 than when k_4^* was set to zero.

The errors in LC′ and LC″ estimated by two different methods are compared in Table 2 using different noise levels and variable input functions. Again, the LC′ was estimated for $k_4^* = 0.01$ using only the first 10 min of an experiment, while LC″ was estimated for k_4^* equal to either zero or 0.01. The mean deviation from the true value obtained for 12 different input functions and the same noise level when applying the conventional method is significantly larger (student t-test, $p < 0.01$) than those estimated by the NLSQ method. An exception to this general conclusion was the mean deviations obtained for the 1% noise and setting k_4^* equal to zero, in which case there was no significant difference found (Table 2).

Animal Study

In experiments where the $C_p^*(t)$ was maintained constant, the coefficient of variation in the $C_p^*(t)$ was between 5.2% and 8.4% throughout 45 min. An example of the $C_p^*(t)$ input function is given in Figure 5. In the lower portion of Figure 5 an example of the NLSQ fit to the g(t) function is shown.

The values for LC, and the whole brain values of k_2^* and k_3^*, estimated from different experimental protocols, are given in Table 3 along with χ_0^2. The LC values obtained with different input function were not influenced by the shape of the input functions when the NLSQ method was applied for data analysis (Table 3).

The mean value of the lumped constant was calculated to be 0.443 ± 0.032. Estimated whole brain transfer constants were 0.124 ± 0.024 and 0.024 ± 0.003 for k_2^* and k_3^*, respectively (Table 3). There was a significant correlation ($N = 45$, $r = 0.96$, $p < 0.001$) between the ratio of ^{18}F concentration in the arterial blood and that in the arterial plasma (Y) with time (X). The linear regression line was $Y = 0.004X + 0.566$. A similar observation was reported before by Phelps et al. (*19*).

DISCUSSION

Sokoloff et al. (*1*) developed a method to determine the lumped constant, the conversion factor essential in converting tissue accumulation of a glucose analog tracer into the tissue utilization of glucose. The method of Sokoloff et al. (*1*) compares equilibrium extraction of glucose and analog in a tissue of interest. The method and the equation used require a constant plasma concentration of the tracer. In measuring lumped and rate constants in different pathologic conditions (*20,21*) we have encountered difficulty in obtaining a constant plasma concentration. Others have also experienced similar difficulty (*4,10,11*). An alternative method for

TABLE 1
Absolute Values of Errors (%) in LC Values Derived for NLSQ and Conventional Method for Various Noise Levels and Different "True" LC Values and Constant Cp* (t) Model*

	NLSQ				Conventional			
Random		LC = 0.25	LC = 0.48	LC = 0.80		LC = 0.25	LC = 0.48	LC = 0.80
	LC′	8.9 ± 7.7	13.5 ± 1.9	5.0 ± 3.4	$k_4^* = 0$	11.6 ± 8.9	4.3 ± 3.3	2.3 ± 1.9
Noise 1%	k_2'	12.2 ± 10.2	3.1 ± 2.9	5.4 ± 4.5	LC″			
	k_3	12.3 ± 13.0	5.8 ± 2.4	5.5 ± 4.8	$k_4^* = 0.01$	10.0 ± 5.7	6.9 ± 5.2	6.6 ± 2.2
	LC′	31.4 ± 23.5	15.0 ± 9.2	8.5 ± 6.8	$k_4^* = 0$	40.5 ± 41.1	33.1 ± 23.9	11.8 ± 0.4
Noise 5%	k_2'	41.0 ± 42.7	21.3 ± 12.4	13.0 ± 8.2	LC″			
	k_3	40.3 ± 30.5	19.0 ± 9.6	17.4 ± 11.1	$k_4^* = 0.01$	67.0 ± 49.6	19.0 ± 15.9	12.0 ± 9.2
	LC′	43.3 ± 43.7	19.1 ± 13.3	8.9 ± 7.7	$k_4^* = 0$	80.7 ± 65.3	59.3 ± 29.1	18.8 ± 15.8
Noise 10%	k_2'	123.1 ± 138.9	40.6 ± 42.3	23.3 ± 11.6	LC″			
	k_3	69.0 ± 56.4	27.9 ± 31.0	17.7 ± 10.4	$k_4^* = 0.01$	119.5 ± 70.0	52.5 ± 37.4	26.6 ± 19.2

Values are means ± s.d.

* Absolute values of the errors (%) in k_2' and k_3' are also shown for the NLSQ method, assuming "true" k_2' and k_3' to be 0.245, and 0.052, respectively.

TABLE 2
Percent Deviations of Estimated LC Values Derived for NLSQ and Conventional Methods for Various Noise Levels and Variable Cp* (t) Models*

	LC′ or LC″														
	NLSQ			Conventional						Rate constants NLSQ					
				Noise 1%		Noise 5%		Noise 10%		Noise 1%		Noise 5%		Noise 10%	
Variation of parameter	Noise 1%	Noise 5%	Noise 10%	$k_4^* = 0$	$k_4^* = 0.01$	$k_4^* = 0$	$k_4^* = 0.01$	$k_4^* = 0$	$k_4^* = 0.01$	$k_2^{*\prime}$	$k_3^{*\prime}$	$k_2^{*\prime}$	$k_3^{*\prime}$	$k_2^{*\prime}$	$k_3^{*\prime}$
100%	−6.8	11.1	−22.2	0.2	−4.6	22.3	−13.5	−40.4	55.2	0.6	−14.5	6.7	10.6	−16.5	−25.3
−50%	−4.1	8.2	−19.5	1.3	8.1	23.3	30.0	−39.4	−31.5	0.9	−1.5	7.9	17.6	−10.4	−13.6
100%	3.9	−2.2	−34.4	4.6	−3.8	−20.0	−12.6	−107.1	56.0	2.5	6.2	5.4	6.3	−42.4	−40.6
−50%	−4.3	5.8	−18.0	0.2	7.3	22.5	29.2	40.3	−32.5	−1.6	−6.2	1.8	7.8	−14.0	−15.3
100%	−2.4	3.4	−14.9	−5.8	9.2	16.5	23.8	−47.1	−38.5	−2.7	0.0	0.0	6.7	−7.2	−6.5
−50%	−5.2	10.7	−19.6	5.6	7.3	27.7	33.9	−34.4	16.7	3.5	−4.3	10.9	15.5	−13.1	−18.0
100%	−7.6	10.8	28.6	11.3	8.1	24.4	16.0	−2.7	60.6	−8.2	−13.0	11.0	−11.4	20.2	15.7
−50%	−2.0	7.5	−15.1	−6.3	1.0	16.0	23.1	47.7	−39.6	8.2	3.1	7.6	17.14	−8.0	−8.4
100%	1.5	−1.9	−14.8	9.6	0.8	−14.8	34.3	−102.4	−26.5	3.3	5.7	5.9	9.0	−9.8	−10.2
−50%	−1.7	11.9	−12.9	−6.3	−10.3	16.3	−19.6	−47.5	49.6	0.0	−3.3	4.6	11.7	−8.4	−7.8
100%	−2.3	−4.9	−15.0	−10.0	−14.2	12.5	19.8	−51.7	−43.3	1.0	−3.0	1.8	5.8	−9.6	−9.9
−50%	3.8	−3.0	−36.9	10.8	14.0	−13.5	35.6	−101.0	−25.0	1.5	5.8	1.4	2.9	−44.0	−42.5
Mean ± s.d. of absolute values	3.8 ±2.0	6.8 ±3.7	21.0 ±8.1	6.0 ±4.0	7.4a ±4.3	19.2b ±4.9	24.3b ±8.2	55.1b ±31.8	39.6b ±13.7	2.8 ±2.7	5.5 ±4.3	5.4 ±3.6	10.2 ±4.7	16.9 ±12.8	17.8 ±12.3

LC′ (NLSQ method) was estimated by assuming $k_4^* = 0.01$, while LC″ (conventional method) was calculated for k_4^* = zero or 0.01. The true LC was assumed to be 0.48. (Student t-test, a: $0.01 < p < 0.05$ b: $p < 0.01$).

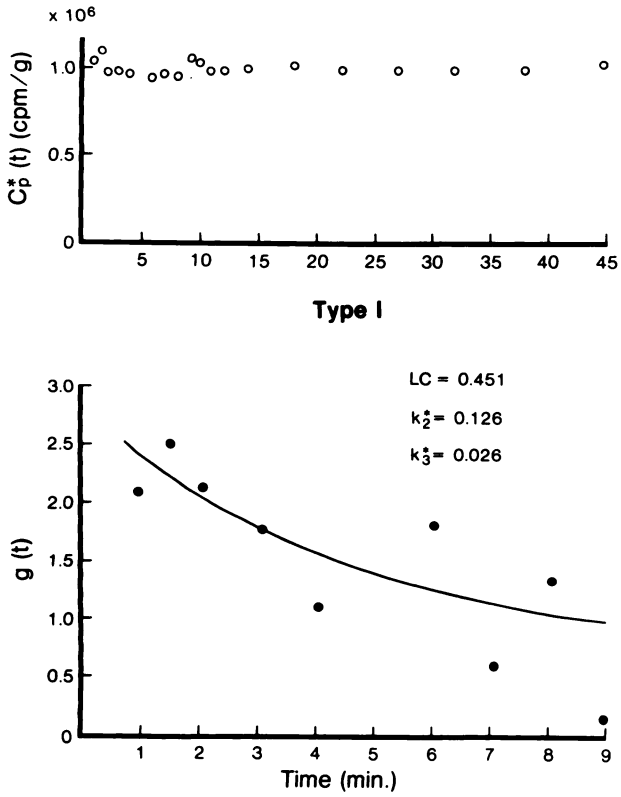

FIGURE 5
Examples of $C_p^*(t)$ (○), g(t) values (●), and model fit to Eq. (A2) (—), using the NLSQ method and constant plasma protocol using [^{18}F]FDG as tracer. The χ_o^2 for the fit was 0.152.

the regional lumped constant determination using carbon-14-labeled 3-O-methyl-D-glucose was decribed (*22*). The method requires several assumptions that are not easily verified, especially in pathologic conditions

TABLE 3
The List of LC, and Whole Brain k_2^* and k_3^* Measured in Cats for 2-[^{18}F]FDG Along with χ_o^2 Values Obtained in NLSQ Fit*

Case	Type of infusion	LC	k_2^* (min-1)	k_3^* (min-1)	Plasma glucose mg/100 ml	χ_o^2
1	I	0.451	0.126	0.026	239	0.152
2	I	0.435	0.107	0.021	180	0.143
3	I	0.400	0.111	0.022	192	0.132
4	I	0.493	0.102	0.021	166	0.083
5	II	0.419	0.128	0.025	161	0.203
6	III	0.471	0.123	0.022	225	0.170
7	IV	0.432	0.173	0.029	159	0.060
Mean		0.443	0.124	0.024	189	
s.d.		0.032	0.024	0.003	32	
s.e.m.		0.012	0.009	0.001	12	

*Following four types of infusion of the tracer were used: constant C_p^* (t) (I): constant C_p^*(t) minus bolus (II): prolonged bolus injection (III): continuous infusion at a constant rate (IV).

(*22*). However, the 3-O-methyl-D-glucose method provides regional information on LC variability.

We describe here a method that allows estimation of the LC in an experimental period of ~10 min without requiring a constant plasma concentration. The method is not dependent on the shape of the input function; however, it is computation-intensive and requires at least a microcomputer to do the calculation. The method uses a NLSQ fitting of experimental data to the model equation yielding information on the LC, and whole-brain rate constants, k_2^* and k_3^*. Since the method requires only 10 min, the assumption of setting $k_4^* = 0$ introduces a very small error (<5% depending on the actual value of k_4^* and the noise level (Fig. 3 and Table 2). An optional experimental time was derived from simulation by assuming different values of k_4^* (an example is given in Fig. 4), noise level, and experimental period. One should note that the 10-min experimental time is only approximate, and depends on the actual value of k_2^*, k_3^*, and k_4^* in the tissue under consideration. Our time, however, compares favorably with that of Reivich et al. (*23*) who noted an optimum experimental period in humans around 20 min using the rate constants for 2-FDG.

The cat brain consists of 50% gray and 50% white matter, the use of one rate constant in these experiments for the calculation of the LC can be easily justified. Sokoloff et al. (*24*) showed that the extraction fraction ratios in their monkey experiment, when analyzed in their entirety, represent a sum of two exponentials. Having the uptake of 2-FDG greater in the gray than in the white matter would also result in an initial period extraction fraction mostly dominated with uptake in the gray matter. This would further justify the use of a single set of the rate constants in the evaluation of the lumped constant.

Since the simulation studies confirmed that the error in LC increases with the noise and duration of the experiment (Fig. 4 and Table 1). The simulation results also suggest that the Sokoloff et al. (*1*) conventional method is more susceptible to the influence of k_4^* (Table 1) than the NLSQ method proposed here. The accuracy of the lumped constant estimated by both methods is also dependent on the absolute value of LC. A trend similar to that outlined above for the LC was found in the accuracy of the rate constants (Table 1). A relevance to our simulation study using LC = 0.8 has been confirmed experimentally in hypoglycemia (*7*) and for an infarcted brain tissue (as high as 2.83) (*5*).

According to Crane et al. (*3*), the theoretical value of the LC for FDG should be much higher than that for DG in rat brain, since both the transport and phosphorylation of FDG are higher than those of DG. However, the values of the LC for FDG obtained in the present study (0.433 ± 0.032) are not significantly different from the previously reported values for DG in

cat brain [0.411 ± 0.013, N = 6, (*2,24*)]. The reason for this is not clear. A comparison of the glucose utilization in the rat brain measured by DG and 2-[^{18}F] FDG indicates that the LC in rat brain for FDG is lower than that for DG (*25*), as Reivich et al. first suggested (*26*).

An ambiguity also exists in the LC values obtained in human brain studies. Reivich et al. (*23*) reported slightly higher values (not significantly different) of the LC for DG than for FDG (0.56 ± 0.043 and 0.52 ± 0.028), respectively. The value measured by the 3-O-methyl glucose method (0.44 ± 0.15) (*5*) was similar to that indirectly estimated by Phelps et al. (*19*) (0.420 ± 0.059).

All these measurements of the lumped constant assume that there is no loss of 2-fluoro-2-deoxy-glucose-6-phosphate. The concentration of glucose-6-phosphatase was believed to be very low in the brain (*27*); however, recent reports (*28,29*) suggest much higher (~30%) dephosphorylation of glucose-6-phosphate. Since the method described here uses data acquired during the first 10 min after the start of injection, the influence, if any, of k_4^* could be ruled out. This conclusion is also supported by unpublished data from this laboratory (Nakai, Matsuda, Diksic, Redies, and Yamamoto) as well as by recent results reported by Nelson et al. (*30*) which indicate that dephosphorylation (k_4^*) does not major influence on data collected up to 40–45 min.

The simulation suggested and the experiment confirmed that the NLSQ method can give more accurate LC values for the whole brain than the conventional method. Unlike the conventional method (*1*), the method described here does not require a constant $C_p^*(t)$. With this technique the whole experiment lasts only ~10 min, the blood loss is reduced, and any type of infusion for the tracer can be used. However, it should be noted that 10-min scans are sufficiently long for a normal cat, while a longer period might be required in pathologic conditions.

NOTES

[+] Palm Springs, CA.

[‡] DuPont Company, No. Billerica, MA.

[§] Model 23A, Yellow Springs Instrument Co., Inc., Yellow Springs, OH.

APPENDIX

Theory

The equation for the LC determination is given by Sokoloff et al. (*1*) as

$$\frac{C_a^*(t) - C_v^*(t)}{C_a - C_v} = \frac{dC_e^*(t)/dt}{R} + \frac{C_e^*(t)}{C_e} \cdot \frac{V_m^* K_m}{\phi\, V_m\, K_m^*}. \quad \text{(A1)}$$

Since in a steady state there is no net accumulation or depletion of glucose, C_e is given (*4,19*) as

$$C_e = \frac{k_1}{k_2 + \phi k_3} C_p, \quad \text{(A2)}$$

and $C_e^*(t)$ can be expressed as (*19*)

$$C_e^*(t) = \frac{k_1^*}{\alpha_2 - \alpha_1} [(k_4^* - \alpha_1)\, e^{-\alpha_1 t} + (\alpha_2 - k_4^*)\, e^{-\alpha_2 t}] \otimes C_p^*(t), \quad \text{(A3)}$$

where

$$\alpha_{1,2} = [k_2^* + k_3^* + k_4^* \mp \sqrt{(k_2^* + k_3^* + k_4^*)^2 - 4k_2^* k_4^*}]/2 \quad \text{(A4)}$$

Dividing Eq. A2 with $C_e^*(t)$, multiplying right side of resultant equation by $[k_1^*/(k_2^* + k_3^*)]/[k_1^*/(k_2^* + k_3^*)]$, and rearranging to obtain $C_e^*(t)/C_e$ expression gives,

$$\frac{C_e^*(t)}{C_e} = \lambda \frac{[(k_2^* + k_3^*)/k_1^*]\, C_e^*(t)}{C_p}, \quad \text{(A5)}$$

where λ is $\dfrac{k_1^*/(k_2^* + k_3^*)}{k_1/(k_2 + \phi k_3)}$, a constant containing rate constants for deoxyglucose and glucose and ϕ.

Substituting Eq. (A5) into Eq. (A1) gives

$$\frac{C_a^*(t) - C_v^*(t)}{C_a - C_v} = \frac{dC_e^*(t)/dt}{R} + \frac{[(k_2^* + k_3^*)/k_1^*]\, C_e^*(t)}{C_p} \cdot \frac{\lambda V_m^* K_m}{\phi V_m K_m^*}, \quad \text{(A6)}$$

where $V_m^* K_m / \phi V_m K_m^*$ is equal to LC. Using an alternative expression for R [Eq. (A7)] derived by Phelps et al. (*19*),

$$R = \frac{C_p\, k_1^* k_3^*}{LC(k_2^* + k_3^*)}, \quad \text{(A7)}$$

Eq. (A6) becomes

$$\frac{C_a^*(t) - C_v^*(t)}{C_a - C_v} = \frac{LC}{C_p}\left[\frac{(k_2^* + k_3^*)}{k_1^* k_3^*} \cdot \frac{dC_e^*(t)}{dt} \cdot \frac{LC(k_2^* + k_3^*)}{C_p\, k_1^*} C_e^*(t)\right]. \quad \text{(A8)}$$

The rate of change of a tracer concentration in the precursor pool, $dC_e^*(t)/dt$, can be expressed as (*19*):

$$\frac{dC_e^*(t)}{dt} = k_1^* C_p^*(t) - (k_2^* + k_3^*)\, C_e^*(t) + k_4^* C_m^*(t), \quad \text{(A9)}$$

where $C_m^*(t)$ as given by Phelps et al. (*19*) is

$$C_m^*(t) = \frac{k_1^* k_3^*}{\alpha_2 - \alpha_1} (e^{-\alpha_1 t} - e^{-\alpha_2 t}) \otimes C_p^*(t). \quad \text{(A10)}$$

Substituting $dC_e^*(t)/dt$ from Eq. (A9) to Eq. (A8) and arranging yields

$$g(t) = \frac{C_p\, (C_a^*(t) - C_v^*(t)}{C_p^*(t)\, (C_a - C_v)} = LC\left(1 + \frac{k_2^*}{k_3^*}\right)\left[1 - \frac{k_2^* C_e^*(t)}{k_1^* C_p^*(t)} + \frac{k_4^* C_m^*(t)}{k_1^* C_p^*(t)}\right]. \quad \text{(A11)}$$

Substituting $C_e^*(t)$ and $C_m^*(t)$ from Eq. (A3) and Eq. (A10), respectively, and arranging yields

$$g(t) = \frac{C_p(C_a^*(t) - C_v^*(t))}{C_p^*(t)\,(C_a - C_v)} = LC\left(1 + \frac{k_2^*}{k_3^*}\right)\left[1 - \frac{(Ae^{-\alpha_1 t} - Be^{-\alpha_2 t}) \otimes C_p^*(t)}{C_p^*(T)\,(\alpha_2 - \alpha_1)}\right], \quad \text{(A12)}$$

where

$$A = k_4^*(k_2^* - k_3^*) - \alpha_1 k_2^* \quad \text{(A13)}$$

$$B = k_4^*(k_2^* - k_3^*) - \alpha_2 k_2^*. \quad \text{(A14)}$$

Equation (A12) expresses g(t), the ratio of extraction fractions for deoxyglucose and glucose in terms of LC, k_2^*, k_3^* (and k_4^*) and the measured $C_p^*(t)$ plasma curve. The use of one set of the rate constants might not be exactly correct because the cat brain consists of 50% gray and 50% white matter. On the other hand, since the purpose is not to determine rate constants and the entire experimental period is only ~10 min, it could be shown that the use of one set of the rate constants will clearly represent the extraction fraction ratios during this initial period even if the function g(t) were a sum of two exponentials with similar half-lives.

ACKNOWLEDGMENTS

This work was supported in part by the Medical Research Council, MA-3174, the Killam Scholarship Fund of the Montreal Neurological Institute, and the Cone Laboratory for Neurosurgical Research. The authors thank Dr. V. Lees for editorial help and Ms. C. Elliott for excellent typing skills.

REFERENCES

1. Sokoloff L, Reivich M, Kennedy C, et al. The ^{14}C deoxyglucose method for measurement of local cerebral glucose utilization: theory, procedure and normal values in the conscious and anesthetized albino rat. *J Neurochem* 1977; 28:897–916.
2. Sokoloff L. Localization of functional activity in the central nervous system by measurement of glucose utilization with radioactive deoxyglucose. *J Cereb Blood Flow Metab* 1981; 1:7–36.
3. Crane PD, Pardridge WM, Braum, LD, et al. Kinetics of transport and phosphorylation of 2-fluoro-2-deoxy-D-glucose in rat brain. *J Neurochem* 1983; 40:160–167.
4. Ginsberg MD, Reivich M. Use of the 2-deoxyglucose method of local cerebral glucose utilization in the abnormal brain: evaluation of the lumped constant during ischemia. *Acta Neurol Scand* 1979; (suppl) 60:226–227.
5. Gjedde A, Wienhard K, Heiss WD, et al. Comparative regional analysis of 2-fluorodeoxyglucose and methylglucose uptake in brain of four stroke patients, with special reference to the regional estimation of the lumped constant. *J Cereb Blood Flow Metab* 1985; 5:163–178.
6. Crane PD, Partridge WM, Braun LP, et al. The interaction of transport and metabolism on brain glucose utilization: a re-evaluation of the lumped constant. *J Neurochem* 1981; 36:1601–1604.
7. Suda S, Shinohara M, Miyaoka M, et al. Local cerebral glucose utilization in hypoglycemia. *J Cereb Blood Flow Metab* 1981; (suppl 1):S62.
8. Schuier F, Orzi F, Suda S, et al. The lumped constant for the ^{14}C deoxyglucose method in hyperglycemic rats. *J Cereb Blood Flow Metab* 1981; (suppl 1):S63.
9. Hawkins RA, Phelps ME, Huang S-C, et al. Effect of ischemia on quantification of local cerebral glucose metabolic rate in man. *J Cereb Blood Flow Metab* 1981; 1:37–51.
10. Kennedy C, Sakurada O, Shinohara M, et al. Local cerebral glucose utilization in the normal conscious macaque monkeys. *Ann Neurol* 1978; 4:293–301.
11. Patlak CS, Pettigrew KD. A method to obtain infusion schedules for prescribed blood concentration time courses. *J Appl Physiol* 1976; 40:458–463.
12. Cunningham VJ, Cremer JL. A method for the simultaneous estimation of regional rates of glucose influx and phosphorylation in rat brain using radiolabelled 2-deoxyglucose. *Brain Res* 1981; 221:319–330.
13. Hawkins RA, Miller AL. Loss of radioactive 2-deoxy-D-glucose-6-phosphate from brains of conscious rats: implications for quantitative autoradiographic determination of regional glucose utilization. *Neuroscience* 1978; 3:251–258.
14. Yeh KC, Kwan KC. A comparison of numerical integrating algorithms by trapezoidal, lagrange, and spline approximation. *J Pharmacokin Biopharm* 1978; 6:79–98.
15. Bevington PR. Least-squares fit to an arbitrary function. In: Bevington PR, ed. Data reduction and error analysis for the physical sciences. New York: McGraw-Hill, 1969:204–246.
16. Fletcher R. A modified Marquardt subroutine for nonlinear least squares. Tech Report AERE R6799, 1971: U.K. Atomic Energy Authority Research Establishment, Harwell, UK.
17. Diksic M, Jolly D. New high-yield synthesis of ^{18}F-labelled 2-deoxy-2-fluoro-D-glucose. *Int J Appl Radiat Isot* 1983; 34:893–896.
18. Adam MJ. A rapid, stereoselective, high yielding synthesis of 2-deoxy-2-fluoro-D-hexopyranase: reaction of glycals with acetyl hypofluorite. *JCS Chem Commun* 1982:730–731.
19. Phelps ME, Huang SC, Hoffman EJ, et al. Tomographic measurement of local cerebral glucose metabolic rate in human with (F-18)2-fluoro-2-deoxy-*D*-glucose: Validation of method. *Ann Neurol* 1979; 6:371–388.
20. Kato A, Diksic M, Yamamoto YL, et al. An improved approach for measurement of regional cerebral rate constants in the deoxyglucose method with positron emission tomography. *J Cereb Blood Flow Metab* 1984; 4:555–563.
21. Kato A, Diksic M, Yamamoto YL, et al. Quantification of glucose utilization in an experimental brain tumor model by the deoxyglucose method. *J Cereb Blood Flow Metab* 1985; 5:108–114.
22. Gjedde A. Calculation of cerebral glucose phosphorylation from brain uptake of glucose analogs in vivo: a re-examination. *Brain Res Rev* 1982; 4:237–274.
23. Reivich M, Alavi A, Wolf A, et al. Glucose metabolic rate kinetic parameter determination in humans: the lumped constants and rate constants for ^{18}F fluorodeoxyglucose and ^{11}C deoxyglucose. *J Cereb Blood Flow Metab* 1985; 5:179–192.

24. Sokoloff L. The ^{14}C deoxyglucose method: Four years later. *Acta Neurol Scand* 1979; (suppl 70) 60:640–649.
25. Sako K, Kato A, Diksic M, et al. Use of short-lived ^{18}F and long-lived ^{14}C in double tracer autoradiography for simultaneous measurement of LCBF and LCGU. *Stroke* 1984; 15:896–900.
26. Reivich M, Kuhl D, Wolf A, et al. The ^{18}F fluorodeoxyglucose method for the measurement of local cerebral glucose utilization in man. *Circ Res* 1979; 44:127–137.
27. Anchors JM, Haggerty DF, Karnovsky ML. Cerebral glucose-6-phosphatase and the movement of 2-deoxy-D-glucose across cell membranes. *J Biol Chem* 1977; 252:7035–7041.
28. Huang MT, Veech RL. The quantitative determination of the in vivo dephosphorylation of glucose-6-phosphate in rat brain. *J Biol Chem* 1982; 257:11358–11363.
29. Huang MT, Veech RL. Metabolic fluxes between ^{14}C 2-deoxy-D-glucose and ^{14}C 2-deoxy-D-glucose-6-phosphate in brain in vivo. *J Neurochem* 1985; 44:567–573.
30. Nelson T, Lucignan G, Atals S, et al. Re-examination of glucose-6-phosphatase activity in the brain in vivo: No evidence for futile cycle. *Science* 1985; 229:60–62.